Oncostatin M renders epithelial cell adhesion molecule-positive liver cancer stem cells sensitive to 5-fluorouracil by inducing hepatocytic differentiation

doi: 10.1158/0008-5472.CAN-09-4210

Title: Oncostatin M renders epithelial cell adhesion molecule-positive liver cancer stem cells sensitive to 5-fluorouracil by inducing hepatocytic differentiation

Running title: Differentiation of EpCAM^{+} Liver CSCs by OSM

Authors: Taro Yamashita, Masao Honda, Kouki Nio, Yasunari Nakamoto, Tatsuya Yamashita, Hiroyuki Takamura, Takashi Tani, Yoh Zen, and Shuichi Kaneko

Affiliation: Center for Liver Diseases, Kanazawa University Hospital, 13-1 Takara-Machi, Kanazawa, Ishikawa 920-8641, Japan

Correspondence: Taro Yamashita, Assistant Professor, Department of Gastroenterology, Kanazawa University Graduate School of Medical Science, 13-1 Takara-Machi, Kanazawa, Ishikawa 920-8641, Japan

Tel: +81-76-265-2851

Fax: +81-76-265-4250

E-mail: taroy@m-kanazawa.jp

Shuichi Kaneko, Director, Center for Liver Diseases, Kanazawa University Hospital; Professor, Department of Gastroenterology, Kanazawa University Graduate School of Medical Science, 13-1 Takara-Machi, Kanazawa, Ishikawa 920-8641, Japan

Tel: +81-76-265-2230

Fax: +81-76-265-4250

E-mail: skaneko@m-kanazawa.jp

Abbreviations: CSCs; cancer stem cells, EpCAM; epithelial cell adhesion molecule, HCC; hepatocellular carcinoma, OSM; Oncostatin M, OSMR; Oncostatin M receptor, STAT3; signal transducer and activator of transcription 3

Abstract

Recent evidence suggests that a certain type of hepatocellular carcinoma (HCC) is hierarchically organized by a subset of cells with stem cell features (cancer stem cells: CSCs). Although normal stem cells and CSCs are considered to share similar self-renewal programs, it remains unclear whether differentiation programs are also maintained in CSCs and effectively utilized for the tumor eradication. In this study, we investigated the effect of oncostatin M (OSM), an interleukin 6-related cytokine known to induce the differentiation of hepatoblasts into hepatocytes, on liver CSCs. OSM receptor (OSMR) expression was detected in the majority of epithelial cell adhesion molecule-positive (EpCAM$^+$) HCC with stem/progenitor cell features. OSM treatment resulted in the induction of hepatocytic differentiation of EpCAM$^+$ HCC cells by inducing signal transducer and activator of transcription 3 activation, as determined by a decrease in stemness-related gene expression, a decrease in EpCAM, α-fetoprotein, and cytokeratin 19 protein expressions, and an increase in albumin protein expression. OSM-treated EpCAM$^+$ HCC cells showed enhanced cell proliferation with expansion of the EpCAM-negative non-CSC population. Noticeably, combination of OSM treatment with the chemotherapeutic agent 5-fluorouracil, which eradicates EpCAM-negative non-CSCs, dramatically increased the number of apoptotic cells *in vitro* and suppressed tumor growth *in vivo* compared with either saline control, OSM, or 5-fluorouracil

treatment alone. Taken together, our data suggest that OSM can be effectively utilized for the differentiation and active cell division of dormant EpCAM$^+$ liver CSCs, and the combination of OSM and conventional chemotherapy with 5-fluorouracil efficiently eliminates HCC by targeting both CSCs and non-CSCs.

Introduction

It is widely accepted that cancer is a disease that develops from a normal cell with accumulated genetic/epigenetic changes. Although considered monoclonal in origin, cancer is composed of heterogeneous cellular populations. These heterogeneities are traditionally explained by the clonal evolution of cancer cells through a series of stochastic genetic events (clonal evolution model) (1). In contrast, cancer cells are known to have the capabilities characteristic of stem cells with respect to self-renewal, limitless division, and generation of heterogeneous cell populations. Recent evidence suggests that tumor cells possess stem cell features (cancer stem cells: CSCs) to self-renew and give rise to relatively differentiated cells through asymmetric division, and thereby form heterogeneous populations (CSC model) (2, 3). Accumulating evidence supports the notion that CSCs can generate tumors more efficiently in immunodeficient mice than non-CSCs in the case of leukemia and various solid tumors (4-9), although the origin of CSCs is still a controversial issue.

Worldwide, hepatocellular carcinoma (HCC) is one of the most common malignancies with poor outcome (10). Recent evidence suggests that at least some HCCs are organized by liver CSCs in a hierarchical manner (11). Several markers have been identified as useful for the enrichment of liver CSCs, including side population

fraction (12), CD133 (13), CD90 (14), and OV6 (15). We have recently utilized epithelial cell adhesion molecule (EpCAM) and α-fetoprotein (AFP) to identify novel prognostic HCC subtypes related to certain developmental stages of human liver lineages (16). Among these, EpCAM-positive ($^+$) AFP$^+$ HCC (hepatic stem cell-like HCC; HpSC-HCC) is characterized by young onset of disease, activation of Wnt/β-catenin signaling, and poor prognosis. *EPCAM* is a target gene of Wnt/β-catenin signaling (17), and we previously identified that EpCAM$^+$ HCC cells from primary HCC samples and cell lines have the features of CSCs, at least in the HpSC-HCC subtype (18). Thus, EpCAM appears to be a potentially useful marker for the isolation of liver CSCs in HpSC-HCC.

CSCs are considered to be resistant to chemotherapy and radiotherapy (19-21), which may be associated with the recurrence of the tumor after treatment. These findings have led to the proposal of 'destemming' CSCs, to induce the differentiation of CSCs into non-CSCs or to eradicate CSCs by inhibiting the signaling pathway responsible for self-renewal (22). Recent studies support this proposal and suggest the utility of bone morphogenic proteins (BMPs), activated during embryogenesis and required for differentiation of neuronal stem cells, to induce differentiation of brain CSCs and facilitate brain tumor eradication (23, 24). However, it is still debatable

whether simple differentiation of CSCs effectively eradicates tumors (25).

Oncostatin M (OSM), an interleukin (IL) 6-related cytokine produced by CD45$^+$ hematopoietic cells, is known to enhance hepatocytic differentiation of hepatoblasts by inducing the activation of the signal transducer and activator of transcription 3 (STAT3) pathway (26). Although OSM, IL6 and leukemia inhibitory factor (LIF) share STAT3 signaling cascades, OSM is known to exploit the distinct hepatocytic differentiation signaling in an OSM receptor (OSMR)-specific manner (27). In this study, we hypothesized that OSM induces hepatocytic differentiation of liver CSCs through the OSMR signaling pathway. We examined OSMR expression and the effect of OSM in EpCAM$^+$ HCC in terms of hepatocytic differentiation and anti-tumor activities.

Materials and Methods

Clinical HCC specimens

A total of 107 HCC tissues and adjacent non-cancerous liver tissues were obtained from patients who underwent hepatectomy for HCC treatment from 1999 to 2007 in Kanazawa University Hospital. These samples were formalin-fixed and paraffin-embedded, and used for immunohistochemistry (IHC). HCC and adjacent non-cancerous liver tissues were histologically diagnosed by two pathologists. An additional fresh EpCAM$^+$ AFP$^+$ HCC sample was obtained from a surgically resected specimen and immediately used for preparation of single-cell suspension and xenotransplantation. All tissue acquisition procedures were approved by the Ethics Committee and the Institutional Review Board of Kanazawa University Hospital. All patients provided written informed consent.

Cell culture and reagents

HuH1 and HuH7 cells were cultured as previously described (18). A primary HCC tissue was dissected and digested in 1 μg/ml type 4 collagenase (Sigma-Aldrich Japan K.K., Tokyo, Japan) solution at 37 °C for 15–30 min. Contaminated red blood cells were lysed with ammonium chloride solution (STEMCELL Technologies, Vancouver, BC, Canada) on ice for 5 min. CD45$^+$ leukocytes and annexin V$^+$ apoptotic cells were

removed by autoMACS-pro cell separator and magnet beads (Miltenyi Biotec K.K., Tokyo, Japan). EpCAM-positive and –negative cells were enriched by autoMACS-pro cell separator and CD326 (EpCAM) MicroBeads (Miltenyi Biotec K.K.). Recombinant OSM was purchased from R&D Systems, Inc. (Minneapolis, MN, USA). 5-Fluorouracil (5-FU) was obtained from Kyowa Kirin (Tokyo, Japan).

Quantitative reverse transcription-polymerase chain reaction (qRT-PCR) analysis

Total RNA was extracted using TRIzol (Invitrogen, Carlsbad, CA, USA) according to the manufacturer's instructions. The expression of selected genes was determined in triplicate using the 7900 Sequence Detection System (Applied Biosystems, Foster City, CA, USA). Each sample was normalized relative to β-actin expression. Probes used were: *TACSTD1*, Hs00158980_m1; *AFP*, Hs00173490_m1; *KRT19*, Hs00761767_s1; *hTERT*, Hs00162669_m1; *Bmi1*, Hs00180411_m1; *POU5F1*, Hs00999632_g1; *CYP3A4*, Hs00430021_m1; *OSMR*, Hs00384278_m1; *ACTB*, Hs99999903_m1 (Applied Biosystems).

Western blotting

Whole cell lysates were prepared using RIPA lysis buffer as described previously (28).

Rabbit polyclonal antibodies to STAT3 (Cell Signaling Technology Inc., Danvers, MA, USA), rabbit polyclonal anti-OSMR antibodies H-200 (Santa Cruz Biotechnology, Santa Cruz, CA, USA), mouse monoclonal anti-phospho-STAT3 (tyr705) antibody (3E2) (Cell Signaling Technology Inc.), and mouse monoclonal anti-β-actin antibody (Sigma-Aldrich) were used. Immune complexes were visualized by enhanced chemiluminescence (Amersham Biosciences Corp., Piscataway, NJ, USA) as described by the manufacturer.

IHC and immunofluorescence (IF) analyses

IHC was performed using Envision+ kits (DAKO, Carpinteria, CA, USA) according to the manufacturer's instructions. Anti-EpCAM monoclonal antibody VU-1D9 (Oncogene Research Products, San Diego, CA, USA) was used for detecting EpCAM. Goat anti-OSMR polyclonal antibodies (C-20) were obtained from Santa Cruz Biotechnology. Mouse anti-CYP3A4 polyclonal antibodies (Abnova, Taipei, Taiwan), mouse anti-CK19 monoclonal antibody (DAKO), and mouse anti-Ki-67 monoclonal antibody MIB-1 (DAKO) were used for detecting CYP3A4, CK19, and Ki-67, respectively. Samples with >5% positive staining in a given area for a particular antibody were considered to be positive. For IF analyses, anti-EpCAM antibody

(Oncogene Research Products), anti-gp130ST antibodies (Santa Cruz Biotechnology), and anti-phospho-STAT3 (tyr705) antibody (3E2) (Cell Signaling Technology Inc.) were used. Alexa 488 fluorescein isothiocyanate (FITC)-conjugated anti-mouse immunoglobulin G (IgG) or Alexa 568 Texas-Red-conjugated anti-goat/rabbit IgG (Molecular Probes) were used as secondary antibodies. Confocal fluorescence microscopic analysis was performed essentially as previously described (18).

Fluorescence-activated cell sorting (FACS) analyses

Cultured cells were trypsinized, washed, and resuspended in Hank's balanced salt solution (Lonza, Basel, Switzerland) supplemented with 1% HEPES and 2% fetal bovine serum (FBS). Cells were then incubated with FITC-conjugated anti-EpCAM monoclonal antibody Clone Ber-EP4 (DAKO) on ice for 30 min, and analyzed using a FACSCalibur (BD Biosciences). Intracellular AFP, cytokeratin (CK) 19, and albumin levels were examined using a BD Cytofix/Cytoperm^{TM} Fixation/Permeabilization Kit (BD Biosciences), anti-AFP mouse monoclonal antibody (Nichirei Biosciences Inc., Tokyo, Japan), anti-CK19 mouse monoclonal antibody (DAKO), and rabbit polyclonal anti- albumin antibodies (Cell Signaling Technology Inc.), respectively.

Cell proliferation and colony formation assay

For cell proliferation assays, 2×10^3 cells were seeded in 96-well plates and cultured with 1% FBS Dulbecco's modified Eagle's meduim (DMEM) (control), 1% DMEM with OSM (100 ng/ml), 5-FU (2 μg/ml), or OSM (100 ng/ml) and 5-FU (2 μg/ml) for 3 to 7 days without media changes. Cell viability was evaluated in quadruplicate using a Cell Titer 96 Aqueous kit (Promega, Madison, WI, USA). For colony formation assay, 1×10^3 cells were harvested in a one-well Culture Slide (BD Biosciences) and cultured with 1% FBS DMEM (control) with or without OSM (100 ng/ml). Culture medium was replaced every 3 days and the colonies were fixed with ice-cold 100% methanol and used for IF 10 days after the initiation of treatment.

RNA interference

SiRNAs specific to OSMR (Silencer® Select SiRNA S17542) and a control siRNA (Silencer® Select Negative Control #1) were obtained from Ambion (Applied Biosystems). To each well of a six-well plate, 2×10^5 cells were seeded 12 hours before transfection. Transfection was performed using Lipofectamine 2000 (Invitrogen), according to the manufacturer's instructions. A total of 100 pM siRNA duplex was used for each transfection.

Apoptosis assay

Cells were cultured in 1% FBS DMEM (control), 1% FBS DMEM with OSM (100 ng/ml), 5-FU (2 μg/ml), or OSM (100 ng/ml) and 5-FU (2 μg/ml) for 3 days in six-well plates or in Culture Slides (BD Biosciences). Annexin V binding to cell membranes was visualized using Annexin V-FITC antibodies and a FACSCalibur flow cytometer (BD Biosciences). Activation of caspase 3 was visualized by IHC or IF using Anti-Active® Caspase-3 polyclonal antibodies (Promega), as described by the manufacturer.

Animal studies

Six-week-old NOD/SCID mice (NOD/NCrCRl-*Prkdc*^{scid}) were purchased from Charles River Laboratories, Inc. (Wilmington, MA, USA). The protocol was approved by the Kanazawa University Animal Care and Use Committee. One million tumor cells were suspended in 200 μl of DMEM and Matrigel (1:1), and a subcutaneous injection was performed. The incidence and size of subcutaneous tumors were recorded. Intratumoral injection of 50 μl of phosphate-buffered saline (PBS; control), OSM (2 μg/tumor), 5-FU (250 μg/tumor), or OSM (2 μg/tumor) and 5-FU (250 μg/tumor) was initiated twice weekly 48 days after injection of tumor cells when the average volume of four tumors in

each group had reached 400 mm^3. For histologic evaluation, tumors were formalin-fixed and paraffin-embedded.

Statistical analyses

The association of OSMR expression and clinicopathologic characteristics in HCC was examined using either Mann-Whitney U or χ^2 tests. Student t-test was used to compare various test groups assayed by qRT-PCR analysis. All analyses were performed using GraphPad Prism software (La Jolla, CA, USA).

Results

Distinct expression of OSMRs in HCC.

Before exploring the effect of OSM on HCC, we examined the expression of its receptor, OSMR, in surgically resected HCC and adjacent non-cancerous liver tissues by IHC. Representative staining of OSMRs in tumor/non-tumor tissues is shown in Figure 1A. In general, cell surface and cytoplasmic immunoreactivity to OSMR was detected rarely in hepatocytes in chronic hepatitis liver (*image a*) but frequently in small hepatocyte-like cells in the stroma or transitional cells in the lobule of cirrhotic liver (*image b*), as indicated by the arrows. Note that immunoreactivity to OSMR was not detected in bile duct epithelia or ductular reactions where EpCAM$^+$ hepatic progenitor cells are thought to accumulate (Supplemental Figure 1), suggesting that OSMRs might be expressed in hepatic progenitor cells committed to hepatocytes. Immunoreactivity to OSMRs was more strongly detected in HCC than in non-cancerous liver (*image c*), and the expression was heterogeneous in the tumor. Of note, OSMRs were detected in HCC cells at the invasive front area of the tumor (*image d*) where CSCs are known to invade frequently (arrows).

Immunoreactivity to OSMR antibodies and EpCAM antibodies was detected in 66 (61.7%) and 38 (35.5%) of 107 HCC specimens, respectively. The clinicopathological characteristics of OSMR$^+$ and -negative ($^-$) HCC cases are shown in

Table 1. OSMR$^+$ HCC was characterized by high serum AFP values (P = 0.009), poorly differentiated morphology (P < 0.0001), and a high frequency of EpCAM$^+$ HCCs (P = 0.024), suggesting that the OSMR is expressed in HCC with stem/progenitor cell features. OSMR$^+$ HCC was also characterized by young onset of disease and male dominance, although these features did not reach statistical significance (P = 0.052 and 0.058, respectively). OSMR was more frequently detected in EpCAM$^+$ HCCs (76.3%) than in EpCAM$^-$ HCCs (53.7%). Expression of OSMR and EpCAM was further investigated by double IF analysis, and immunoreactivity to OSMR was detected in both EpCAM$^+$ normal hepatic progenitors (Figure 1B) and EpCAM$^+$ HCC cells (Figure 1C). These data suggest that although OSMR is more widely expressed than EpCAM in HCC, OSMR is frequently expressed in EpCAM$^+$ normal hepatic progenitors and liver CSCs.

OSM induces hepatocytic differentiation of EpCAM$^+$ HCC.

Because OSMR was expressed in the majority of EpCAM$^+$ HCCs, we investigated the effect of OSM on EpCAM$^+$ HCC cell lines. First, we examined the expression of OSMR and its signal transducer glycoprotein 130 (gp130) in EpCAM$^+$ AFP$^+$ HCC cell lines HuH1 and HuH7 by IF (Figure 2A). Both gp130 and OSMR protein expressions were

detected in these cells, consistent with the IHC data. Because OSM is known to induce the hepatocytic differentiation of hepatoblasts in a STAT3-dependent manner, we investigated the effect of OSM on phospholyration of STAT3 in HuH1 and HuH7 cells by IF and Western blotting. Incubation of HCC cells for 1 hour with OSM at a concentration of 100 ng/ml resulted in the induction and nuclear accumulation of phospholyrated STAT3 (pSTAT3) compared with the control (Figure 2B and 2C). We examined the effect of OSM on the EpCAM$^+$ cell population in HuH1 and HuH7 cells. We first labeled HuH1 and HuH7 cells with CD326 (EpCAM) MicroBeads and FITC-conjugated anti-EpCAM antibodies (Clone Ber-EP4) and performed positive/negative selection using magnetic activated cell sorting (MACS) to determine the appropriate gating criteria for EpCAM-high (designated as EpCAM$^+$) and –low/negative (designated as EpCAM$^-$) cell population (Figure 2D upper panels). It is interesting that OSM treatment (100 ng/ml for 72 hours) diminished the EpCAM$^+$ cell population from 50.7% to 10.1% in HuH1 and from 55.2% to 28.8% in HuH7 cells when the same constant gating criteria was applied (Figure 2D lower panels).

We used RNA interference to investigate whether the decrease in EpCAM$^+$ cells by OSM treatment depends on the expression of OSMR. Transfection of siRNAs specific to *OSMR* (Si-OSMR) resulted in the knockdown of target genes compared with

the control (Si-Control) in HuH1 and HuH7 cells 48 hours after transfection (Supplemental Figure 2A). We further confirmed the decrease of OSMR protein expression by IF and Western blotting 72 hours after transfection (Supplemental Figure 2B and 2C). When we treated these HuH1 and HuH7 cells with OSM (100 ng/ml) for 1 hour, we observed the decrease of pSTAT3 by *OSMR* gene silencing compared with the control (Supplemental Figure 2C). Furthermore, OSM-mediated decrease in the number of EpCAM$^+$ cells was inhibited by *OSMR* gene silencing (Supplemental Figure 2D), suggesting that OSM exploits the diminution of EpCAM$^+$ cells through the activation of the OSMR signaling pathway in EpCAM$^+$ HCC.

We further examined the effect of OSM on hepatocytic differentiation by qRT-PCR and FACS analyses. OSM treatment in HuH1 cells reduced the expression of hepatic progenitor -related genes including *AFP*, *KRT19* (encoding CK19), and *TERT* (encoding telomerase reverse transcriptase; TERT) (Figure 3A). OSM treatment further reduced the expression of *BMI1* and *POU5F1* (encoding Oct4), which is known to be expressed and required for self-renewal in embryonic stem cells. OSM treatment also increased the expression of the hepatocyte marker *CYP3A4*. Furthermore, OSM treatment reduced AFP$^+$ and CK19$^+$ cells and increased albumin$^+$ cells compared with the untreated control, as evaluated by the geometric mean of the fluorescence intensities

of whole cells analyzed by intracellular FACS (Figure 3B). Similar results were obtained in HuH7 cells (data not shown) and, taken together, these data suggest that OSM induced the hepatocytic differentiation of EpCAM$^+$ HCCs.

Hepatocytic differentiation of EpCAM$^+$ HCC by OSM augments cell proliferation.

In general, normal stem cells are more quiescent than differentiated cells in terms of cell division. We therefore evaluated the effect of OSM on cell proliferation in HuH1 and HuH7 cells. It is interesting that OSM treatment for 10 days resulted in the larger colony formation following treatment with OSM (100 ng/ml) than the untreated control. Of note, the majority of cells comprising these larger colonies was EpCAM$^-$, or had low expression levels, whereas a subset of untreated control cells maintained high EpCAM expression (Figure 3C). Similar results were obtained when cell proliferation was examined using an (3-(4, 5-dimethylthiazol-2-yl)-5-(3-carboxymethoxyphenyl)-2-(4-sulfophenyl)-2H-tetrazolium) tetrazolium (MTS) assay and Ki-67 labeling index (Figure 3D). OSM modestly enhanced cell proliferation (upper panels) and increased Ki-67-positive cells (middle and lower panels) compared with the untreated control in both HuH1 and HuH7 cells with statistical significance (Figure 3D).

OSM treatment increases chemosensitivity of EpCAM$^+$ HCC.

The above-mentioned data imply that although OSM may induce the hepatocytic differentiation of dormant EpCAM$^+$ liver CSCs, OSM treatment alone may instead enhance cell proliferation through expansion of amplifying differentiated cancer cells *in vitro*, raising the question of efficacy of differentiation therapy in EpCAM$^+$ HCC. Because rapidly amplifying cells are considered to be more sensitive to chemotherapeutic agents, we investigated the effect of combining OSM treatment with conventional chemotherapy to target both dormant CSCs and amplifying non-CSCs. We have shown that 5-FU treatment alone can diminish EpCAM$^-$ non-CSCs that result in the enrichment of EpCAM$^+$ CSCs in HCC (18). We therefore explored the effect of 5-FU in combination with OSM on EpCAM$^+$ HCC cell proliferation and apoptosis *in vitro*.

When HuH1 and HuH7 cells were treated with OSM alone and cultured for 7 days, cell proliferation was modestly increased compared with the untreated control (Figure 4A). In contrast, 5-FU treatment clearly inhibited cell proliferation. Noticeably, combination of OSM and 5-FU effectively suppressed cell proliferation in HuH1 and HuH7 cells (Figure 4A). We further investigated the effects of OSM and 5-FU on

apoptosis, evaluated by annexin V binding to cell membranes and the activation of caspase 3 (Figure 4B and C). Although OSM treatment alone had a small effect on induction of apoptosis, 5-FU treatment induced annexin-V$^+$ and activated caspase 3$^+$ cells more than in the control. Combination of OSM and 5-FU most strongly induced apoptosis in both HuH1 and HuH7 cells with statistical significance.

Finally, we investigated the effect of OSM on EpCAM$^+$ HCC *in vivo* using a primary HCC specimen and cell lines. Single-cell suspensions from primary EpCAM$^+$ HCC cells (1×10^6 cells) were injected into 6-week-old male NOD/SCID mice, and these cells formed subcutaneous tumors 48 days after transplantation. Subsequently, 50 μl of PBS, OSM (2 μg/tumor), 5-FU (250 μg/tumor), or OSM (2 μg/tumor) and 5-FU (250 μg/tumor) solution were injected directly in each tumor twice a week. Although OSM treatment alone showed weak tumor suppressive effects, the changes in tumor size demonstrated no significant difference compared with the control (Figure 5A). Similarly, 5-FU treatment alone showed limited tumor suppressive effects. However, combination of OSM with 5-FU showed marked inhibition of tumor growth compared with PBS control or 5-FU alone (P = 0.02 and 0.05, respectively). IHC analysis of xenografted tumors showed that OSM treatment decreased the number of EpCAM$^+$ or CK19$^+$ cells and increased CYP3A4$^+$ cells *in vivo* (Supplemental Figure 3A and 3B). FACS analysis

of xenografted tumors further confirmed the decrease of EpCAM$^+$ cell population by OSM treatment *in vivo* (Supplemental Figure 3C). IHC analysis revealed that combination of OSM with 5-FU strongly induced the activation of caspase 3 compared with PBS control, OSM, or 5-FU (Figure 5B). Taken together, these data suggest that hepatocytic differentiation of EpCAM$^+$ HCC cells induced by OSM was the most effective for inhibition of tumor growth *in vivo* when the conventional chemotherapeutic agent 5-FU was co-administered.

Discussion

A growing body of evidence suggests that there are similarities between normal stem cells and CSCs in terms of self-renewal programs (29). We have recently reported that Wnt/β-catenin signaling augments the self-renewal and inhibits the differentiation of EpCAM$^+$ liver CSCs (18). In the present study, we have shown that the OSM–OSMR signaling pathway is maintained in HCCs with stem/progenitor cell features. OSM induces the hepatocytic differentiation and activates cell division in dormant EpCAM$^+$ liver CSCs (Figure 5C). Furthermore, we have demonstrated that combination of OSM and 5-FU effectively inhibits tumor cell growth, revealing the importance of targeting both CSCs and non-CSCs for eradication of the tumor.

OSM is a pleiotropic cytokine that belongs to the IL-6 family that includes IL6, IL11, and LIF. These cytokines share the gp130 receptor subunit as a common signal transducer, and activate Janus tyrosine kinases and the STAT3 pathway. However, gp130 forms a heterodimer with a unique partner such as the IL6 receptor, LIF receptor, or OSMR, thus transducing a certain signaling uniquely induced by each cytokine (30). Of note, OSM is known to activate hepatocytic differentiation programs in hepatoblasts in an OSMR-specific manner (27), and our data demonstrated that OSM can induce hepatocytic differentiation and active cell proliferation in EpCAM$^+$ HCC through OSMR signaling.

OSMR is expressed in hepatoblasts in the fetal liver (26). We have found that OSMR is frequently expressed in normal hepatic progenitors but is rarely detected in hepatocytes in adult livers. Interestingly, OSMR$^+$ HCC was characterized by high serum AFP, frequent EpCAM positivity, and poorly differentiated morphology, suggesting that OSMR is more likely expressed in HCC with stem/progenitor cell features (16). Although the regulatory mechanisms of OSMR are still unclear, it is plausible that OSMR expression is regulated by a signaling pathway activated during the process of hepatogenesis. Because gp130 is known to be ubiquitously expressed, regulation of OSM signaling may be largely dependent on the expression status of OSMR in normal and tumor tissues. Recent studies have demonstrated the potential role of methylation of CpG islands located in OSMR promoter in colorectal cancer (31, 32). Clarification of OSMR promoter activity regulation including CpG methylation may provide clues for better understanding of hepatocytic differentiation signaling in both normal hepatic stem cells and CSCs.

It has been postulated that both normal stem cells and CSCs are dormant and show slow cell cycles. Consistent with this, CSCs are considered to be more resistant to chemotherapeutic agents than non-CSCs possibly due to slow cell cycles as well as an increased expression of ATP-binding cassette transporters, robust DNA damage

responses, and activated anti-apoptotic signaling (20, 33, 34). Therefore, development of an effective strategy by targeting CSC pools together with conventional chemotherapies is essential to eradicate a tumor mass. Two strategies have been investigated to reduce the CSCs population in the tumor; that is, inhibition of self-renewal programs and activation of differentiation programs. We have demonstrated that hepatocytic differentiation of liver CSCs by OSM results in enhanced cell proliferation *in vitro*. We have further shown here that OSM-mediated hepatocytic differentiation of liver CSCs in combination with conventional chemotherapy effectively suppresses HCC growth. It is possible that OSM may boost anti-tumor activity of 5-FU by “exhausting dormant CSCs” through hepatocytic differentiation and active cell division. It is encouraging that similar success with differentiation therapy has recently been reported in several cancers (24, 35, 36). In addition, HNF4-α-mediated differentiation of HCC cells has recently been reported to be effective for eradication of HCC (37). However, although combination of OSM and 5-FU effectively inhibited the tumor growth in our model, we could not observe the shrinkage of the tumor. Thus, induction of CSC’s differentiation with eradication of non-CSCs might not be enough for eradication of the tumor, which may suggest the importance of inhibiting self-renewal as well as stimulating differentiation of CSCs.

Because we induced the hepatocytic differentiation of the subcutaneous tumor by local injection of OSM, further rigorous studies are clearly required to assess the effect of OSM on liver CSCs and its utility for differentiation therapy in HCC.

CSCs may acquire resistance against differentiation therapy by additional genetic/epigenetic changes during treatment by clonal evolution, as observed in conventional chemotherapy. Indeed, it has recently been suggested that BMP-mediated brain CSC differentiation failed in a subset of brain tumors in which BMP receptor promoters were methylated and silenced (23). Similarly, OSMR silencing by promoter methylation may result in the development of OSM-resistant clones in HCC.

In conclusion, OSMR is expressed in certain types of HCC with stem/progenitor cell features, and OSM induces hepatocytic differentiation and active cell division of OSMR$^+$ liver CSCs to enhance chemosensitivity to 5-FU. The clinical safety and utility of OSM should be evaluated in the near future.

Acknowledgments

Grant Support: This study was supported by a Grant-in-Aid from the Ministry of Education, Culture, Sports, Science and Technology, Japan (No. 20599005).

We thank Ms. Masayo Baba and Ms. Nami Nishiyama for excellent technical

assistance.

References

1. Fialkow PJ. Clonal origin of human tumors. Biochim Biophys Acta 1976; 458: 283-321.
2. Clarke MF, Dick JE, Dirks PB, et al. Cancer stem cells--perspectives on current status and future directions: AACR Workshop on cancer stem cells. Cancer Res 2006; 66: 9339-44.
3. Jordan CT, Guzman ML, Noble M. Cancer stem cells. N Engl J Med 2006; 355: 1253-61.
4. Al-Hajj M, Wicha MS, Benito-Hernandez A, Morrison SJ, Clarke MF. Prospective identification of tumorigenic breast cancer cells. Proc Natl Acad Sci U S A 2003; 100: 3983-8.
5. Bonnet D, Dick JE. Human acute myeloid leukemia is organized as a hierarchy that originates from a primitive hematopoietic cell. Nat Med 1997; 3: 730-7.
6. O'Brien CA, Pollett A, Gallinger S, Dick JE. A human colon cancer cell capable of initiating tumour growth in immunodeficient mice. Nature 2007; 445: 106-10.
7. Ricci-Vitiani L, Lombardi DG, Pilozzi E, et al. Identification and expansion of human colon-cancer-initiating cells. Nature 2007; 445: 111-5.
8. Singh SK, Hawkins C, Clarke ID, et al. Identification of human brain tumour initiating cells. Nature 2004; 432: 396-401.
9. Visvader JE, Lindeman GJ. Cancer stem cells in solid tumours: accumulating evidence and unresolved questions. Nat Rev Cancer 2008; 8: 755-68.
10. El-Serag HB, Rudolph KL. Hepatocellular carcinoma: epidemiology and molecular carcinogenesis. Gastroenterology 2007; 132: 2557-76.
11. Mishra L, Banker T, Murray J, et al. Liver stem cells and hepatocellular carcinoma. Hepatology 2009; 49: 318-29.
12. Chiba T, Kita K, Zheng YW, et al. Side population purified from hepatocellular carcinoma cells harbors cancer stem cell-like properties. Hepatology 2006; 44: 240-51.
13. Ma S, Chan KW, Hu L, et al. Identification and characterization of tumorigenic liver cancer stem/progenitor cells. Gastroenterology 2007; 132: 2542-56.
14. Yang ZF, Ho DW, Ng MN, et al. Significance of CD90+ cancer stem cells in human liver cancer. Cancer Cell 2008; 13: 153-66.
15. Yang W, Yan HX, Chen L, et al. Wnt/beta-catenin signaling contributes to activation of normal and tumorigenic liver progenitor cells. Cancer Res 2008; 68: 4287-95.

16. Yamashita T, Forgues M, Wang W, et al. EpCAM and alpha-fetoprotein expression defines novel prognostic subtypes of hepatocellular carcinoma. Cancer Res 2008; 68: 1451-61.
17. Yamashita T, Budhu A, Forgues M, Wang XW. Activation of hepatic stem cell marker EpCAM by Wnt-beta-catenin signaling in hepatocellular carcinoma. Cancer Res 2007; 67: 10831-9.
18. Yamashita T, Ji J, Budhu A, et al. EpCAM-positive hepatocellular carcinoma cells are tumor-initiating cells with stem/progenitor cell features. Gastroenterology 2009; 136: 1012-24.
19. Boman BM, Huang E. Human colon cancer stem cells: a new paradigm in gastrointestinal oncology. J Clin Oncol 2008; 26: 2828-38.
20. Dean M, Fojo T, Bates S. Tumour stem cells and drug resistance. Nat Rev Cancer 2005; 5: 275-84.
21. Zou GM. Cancer initiating cells or cancer stem cells in the gastrointestinal tract and liver. J Cell Physiol 2008; 217: 598-604.
22. Hill RP, Perris R. "Destemming" cancer stem cells. J Natl Cancer Inst 2007; 99: 1435-40.
23. Lee J, Son MJ, Woolard K, et al. Epigenetic-mediated dysfunction of the bone morphogenetic protein pathway inhibits differentiation of glioblastoma-initiating cells. Cancer Cell 2008; 13: 69-80.
24. Piccirillo SG, Reynolds BA, Zanetti N, et al. Bone morphogenetic proteins inhibit the tumorigenic potential of human brain tumour-initiating cells. Nature 2006; 444: 761-5.
25. Nasr R, Guillemin MC, Ferhi O, et al. Eradication of acute promyelocytic leukemia-initiating cells through PML-RARA degradation. Nat Med 2008; 14: 1333-42.
26. Kamiya A, Kinoshita T, Ito Y, et al. Fetal liver development requires a paracrine action of oncostatin M through the gp130 signal transducer. EMBO J 1999; 18: 2127-36.
27. Kinoshita T, Miyajima A. Cytokine regulation of liver development. Biochim Biophys Acta 2002; 1592: 303-12.
28. Yamashita T, Honda M, Takatori H, et al. Activation of lipogenic pathway correlates with cell proliferation and poor prognosis in hepatocellular carcinoma. J Hepatol 2009; 50: 100-10.
29. Lobo NA, Shimono Y, Qian D, Clarke MF. The biology of cancer stem cells. Annu Rev Cell Dev Biol 2007; 23: 675-99.
30. Heinrich PC, Behrmann I, Haan S, Hermanns HM, Muller-Newen G, Schaper F.

Principles of interleukin (IL)-6-type cytokine signalling and its regulation. Biochem J 2003; 374: 1-20.

31. Deng G, Kakar S, Okudiara K, Choi E, Sleisenger MH, Kim YS. Unique methylation pattern of oncostatin m receptor gene in cancers of colorectum and other digestive organs. Clin Cancer Res 2009; 15: 1519-26.

32. Kim MS, Louwagie J, Carvalho B, et al. Promoter DNA methylation of oncostatin m receptor-beta as a novel diagnostic and therapeutic marker in colon cancer. PLoS ONE 2009; 4: e6555.

33. Bao S, Wu Q, McLendon RE, et al. Glioma stem cells promote radioresistance by preferential activation of the DNA damage response. Nature 2006; 444: 756-60.

34. Viale A, De Franco F, Orleth A, et al. Cell-cycle restriction limits DNA damage and maintains self-renewal of leukaemia stem cells. Nature 2009; 457: 51-6.

35. Gupta PB, Onder TT, Jiang G, et al. Identification of selective inhibitors of cancer stem cells by high-throughput screening. Cell 2009; 138: 645-59.

36. Sipkins DA. Rendering the leukemia cell susceptible to attack. N Engl J Med 2009; 361: 1307-9.

37. Yin C, Lin Y, Zhang X, et al. Differentiation therapy of hepatocellular carcinoma in mice with recombinant adenovirus carrying hepatocyte nuclear factor-4alpha gene. Hepatology 2008; 48: 1528-39.

Figure legends

Figure 1. (A) Representative images of OSMR staining in non-cancerous liver tissues and HCC tissues. Immunoreactivity to OSMR was not detected in hepatocytes in chronic hepatitis liver tissue (*image a*) but was detected in a subset of small hepatocyte-like cells in the stroma or transitional cells in the lobule (*image b*, arrows) of cirrhotic liver tissue. OSMR was more abundantly expressed in HCC than in non-cancerous liver (*image c*). OSMR$^+$ cancer cells were disseminated in the invasive front area of the tumor (*image d*, arrows). PT: portal tract, BD: bile duct. **(B and C)** Double IF analysis of EpCAM (green) and OSMR (red) expression in non-cancerous **(B)** and HCC **(C)** tissues.

Figure 2. (A) IF analysis of gp130 and OSMR expression in HuH1 and HuH7 cell lines. **(B)** IF analysis of phospholyrated STAT3 expression in HuH1 and HuH7 cell lines stimulated by OSM (100 ng/ml for 1 hour) and controls. **(C)** Western blotting analysis of whole or phospholyrated STAT3 protein expression in HuH1 and HuH7 cells stimulated by OSM (100 ng/ml for 1 hour), and controls. **(D)** FACS analysis of HuH1 and HuH7 cells stained with FITC-conjugated anti-EpCAM antibodies. Upper panels: EpCAM-high (designated as EpCAM$^+$) (yellow) and -low/negative cells (designated as

EpCAM$^-$) (blue) were enriched by MACS and labeled with FITC-conjugated anti-EpCAM antibodies or isotype control antibodies. Lower panels: Cells were cultured in 1% FBS DMEM with (green) or without OSM (100 ng/ml) (orange) for 3 days and stained with FITC-conjugated anti-EpCAM antibodies.

Figure 3. (A) qRT-PCR analysis of HuH1 cells cultured in 1% FBS DMEM with (black bar) or without (white bar) OSM (100 ng/ml) for 3 days. **(B)** Intracellular FACS analysis of HuH1 cells cultured in 1% FBS DMEM with (green line) or without (red line) OSM (100 ng/ml) for 3 days. The number in the figure indicates the geometric mean of the fluorescence intensity on a logarithmic scale. **(C)** IF analysis of HuH1 and HuH7 cell colonies cultured in 1% FBS DMEM with or without OSM (100 ng/ml) for 10 days. Colonies were fixed with 100% ice-cold methanol and stained with FITC-conjugated anti-EpCAM antibodies. **(D)** Upper panels: Cell proliferation assay of HuH1 and HuH7 cells cultured in 1% FBS DMEM with (black bar) or without (white bar) OSM (100 ng/ml) for 3 days. Middle and lower panels: IF analysis of HuH1 and HuH7 cells cultured in 1% FBS DMEM with or without OSM (100 ng/ml) for 3 days. Cells were fixed with 100% ice-cold methanol and stained with anti-Ki-67 antibodies.

Figure 4. (A) Cell proliferation assay of HuH1 and HuH7 cells cultured in 1% FBS DMEM with OSM (100 ng/ml) (light gray bar), 5-FU (2 μg/ml) (gray bar), OSM (100 ng/ml) and 5-FU (2 μg/ml) (black bar), or PBS as control (white bar) for 7 days. **(B)** FACS analysis of HuH1 and HuH7 cells stained with FITC-conjugated anti-Annexin V antibodies. Cells were cultured in 1% FBS DMEM with OSM (100 ng/ml) (green line), 5-FU (2 μg/ml) (blue line), OSM (100 ng/ml) and 5-FU (2 μg/ml) (red line), or PBS as control (gray line) for 3 days. **(C)** Left panels: IF analysis of HuH1 and HuH7 cells stained with anti-active-caspase 3 antibodies. Cells were cultured in 1% FBS DMEM with OSM (100 ng/ml), 5-FU (2 μg/ml), OSM (100 ng/ml) and 5-FU (2 μg/ml), or PBS control for 3 days. Right panels: Bar graphs indicating the percentages of active-caspase 3 positive cells.

Figure 5. (A) Effect of PBS, OSM, 5-FU, and OSM plus 5-FU injections on the growth of primary EpCAM$^+$ AFP$^+$ HCC xenograft tumors in NOD/SCID mice (n = 4 in each group). Intratumoral injection of 50 μl PBS, OSM (2 μg/tumor), 5-FU (250 μg/tumor), or OSM (2 μg/tumor) and 5-FU (250 μg/tumor) was initiated 48 days after transplantation twice per week. **(B)** Representative images of activated caspase 3 staining of xenograft tumors in each treatment group (PBS: *image a*, OSM: *image b*,

5-FU: *image c*, OSM and 5-FU, *image d*). **(C)** A schematic diagram of the effect of OSM on EpCAM$^+$ liver CSCs. Dormant EpCAM$^+$ liver CSCs with OSMR expression respond to OSM and differentiate into rapidly dividing EpCAM$^-$ non-CSCs that are highly sensitive to 5-FU.

Table 1. Clinicopathological characteristics of $OSMR^+$ and $OSMR^-$ HCC cases used for IHC analyses

Parameters	$OSMR^+$ (n = 66)	$OSMR^-$ (n = 41)	*P*-value*
Age (years, mean ± SE)	62.7 ± 1.3	66.4 ± 1.3	0.052
Sex (male/female)	55/11	27/14	0.058
Etiology (HBV/HCV/other)	25/35/6	8/30/3	0.10
Liver cirrhosis (yes/no)	43/23	26/15	1.0
AFP (ng/ml, mean ± SE)	6453 ± 5901	1039 ± 935	0.009
Histological grade**			
I-II	3	16	
II-III	54	20	
III-IV	9	5	<0.0001
Tumor size (<3cm/>3cm)	30/36	15/26	0.42
TNM classification			
I/II	48	31	
III/IV	18	10	0.82
EpCAM (positive/negative)	29/37	9/32	0.024

*Mann-Whitney U test or χ^2 test

**Edmondson-Steiner

Supplemental Figure Legends

Supplemental Figure 1. Double IF analysis of EpCAM (green) and OSMR (red) expression in non-cancerous liver. Small hepatocyte-like cells in the lobule expressed both EpCAM and OSMR (yellow arrows), whereas epithelial cells in ductular reaction expressed EpCAM (green arrows) but not OSMR.

Supplemental Figure 2. (A) qRT-PCR analysis of *OSMR* gene expression in HuH1 and HuH7 cells 48 hours after transfection with Si-Control (white bar) or Si-OSMR (gray bar). **(B)** IF analysis of OSMR expression in HuH1 cells 72 hours after transfection with Si-Control or Si-OSMR. **(C)** Western blotting analysis of OSMR, phospho-STAT3 and beta actin expression in HuH1 and HuH7 cells 72 hours after transfection with Si-Control or Si-OSMR. Cells were treated with OSM (100 ng/ml) for 1 hour before cell lysis. **(D)** FACS analysis of HuH1 cells stained with FITC-conjugated anti-EpCAM antibodies. Twenty-four hours after transfection with each siRNA, cells were cultured in 1% FBS DMEM with or without OSM (100 ng/ml) for 72 hours.

Supplemental Figure 3. (A) Representative images of EpCAM, CYP3A4, and CK19

staining of xenograft tumors treated with OSM (2 μg/tumor) or PBS as control. **(B)** A bar graph indicating the percentages of CK19-positive cells in xenograft tumors treated with OSM (2 μg/tumor) (black) or PBS (white) as control. **(C)** FACS analysis of xenograft tumor cells treated with OSM (2 μg/tumor) or PBS and stained with FITC-conjugated anti-EpCAM antibodies or isotype control.

Figure 1

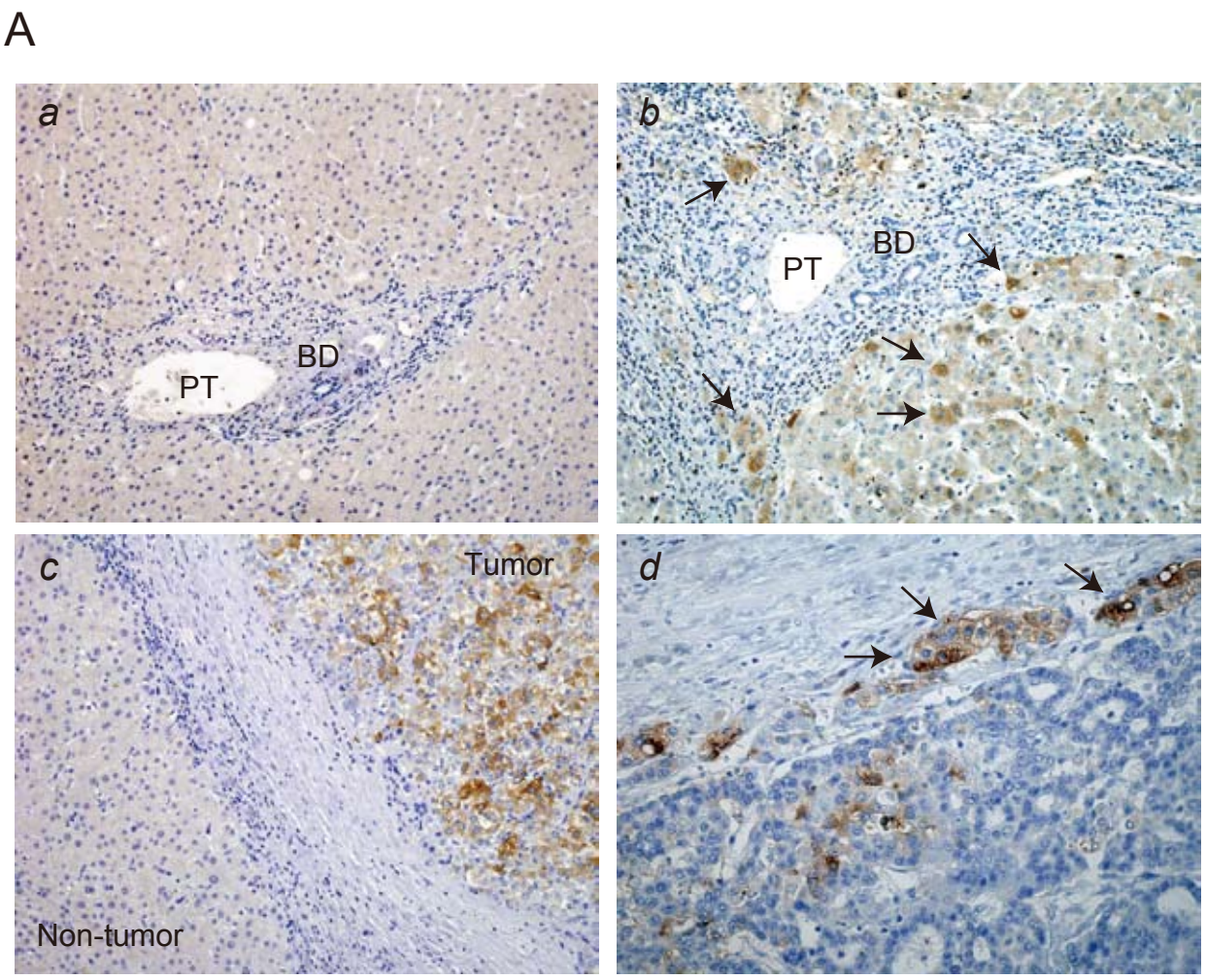
A
a
PT
BD
b
PT
BD
c
Tumor
Non-tumor
d
B
EpCAM
OSMR
DAPI
Merge
C
EpCAM
OSMR
DAPI
Merge

Figure 2

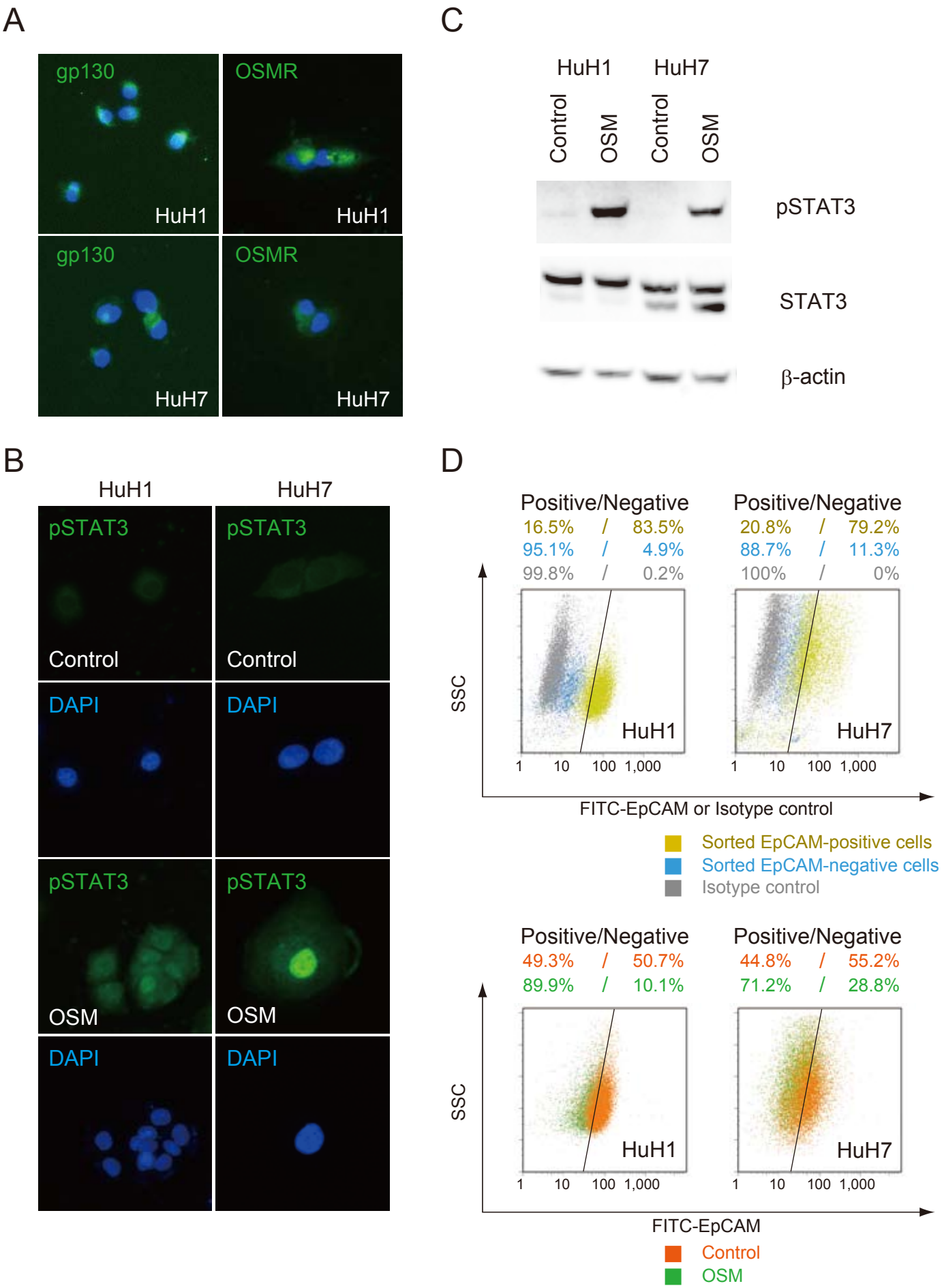
A
gp130
OSMR
HuH1
HuH1
gp130
OSMR
HuH7
HuH7
B
HuH1
HuH7
pSTAT3
pSTAT3
Control
Control
DAPI
DAPI
pSTAT3
pSTAT3
OSM
OSM
DAPI
DAPI
C
HuH1
HuH7
Control
OSM
Control
OSM
pSTAT3
STAT3
β-actin
D
Positive/Negative
16.5% / 83.5%
95.1% / 4.9%
99.8% / 0.2%
Positive/Negative
20.8% / 79.2%
88.7% / 11.3%
100% / 0%
SSC
HuH1
HuH7
1 10 100 1,000
1 10 100 1,000
FITC-EpCAM or Isotype control
Sorted EpCAM-positive cells
Sorted EpCAM-negative cells
Isotype control
Positive/Negative
49.3% / 50.7%
89.9% / 10.1%
Positive/Negative
44.8% / 55.2%
71.2% / 28.8%
SSC
HuH1
HuH7
1 10 100 1,000
1 10 100 1,000
FITC-EpCAM
Control
OSM

Figure 3

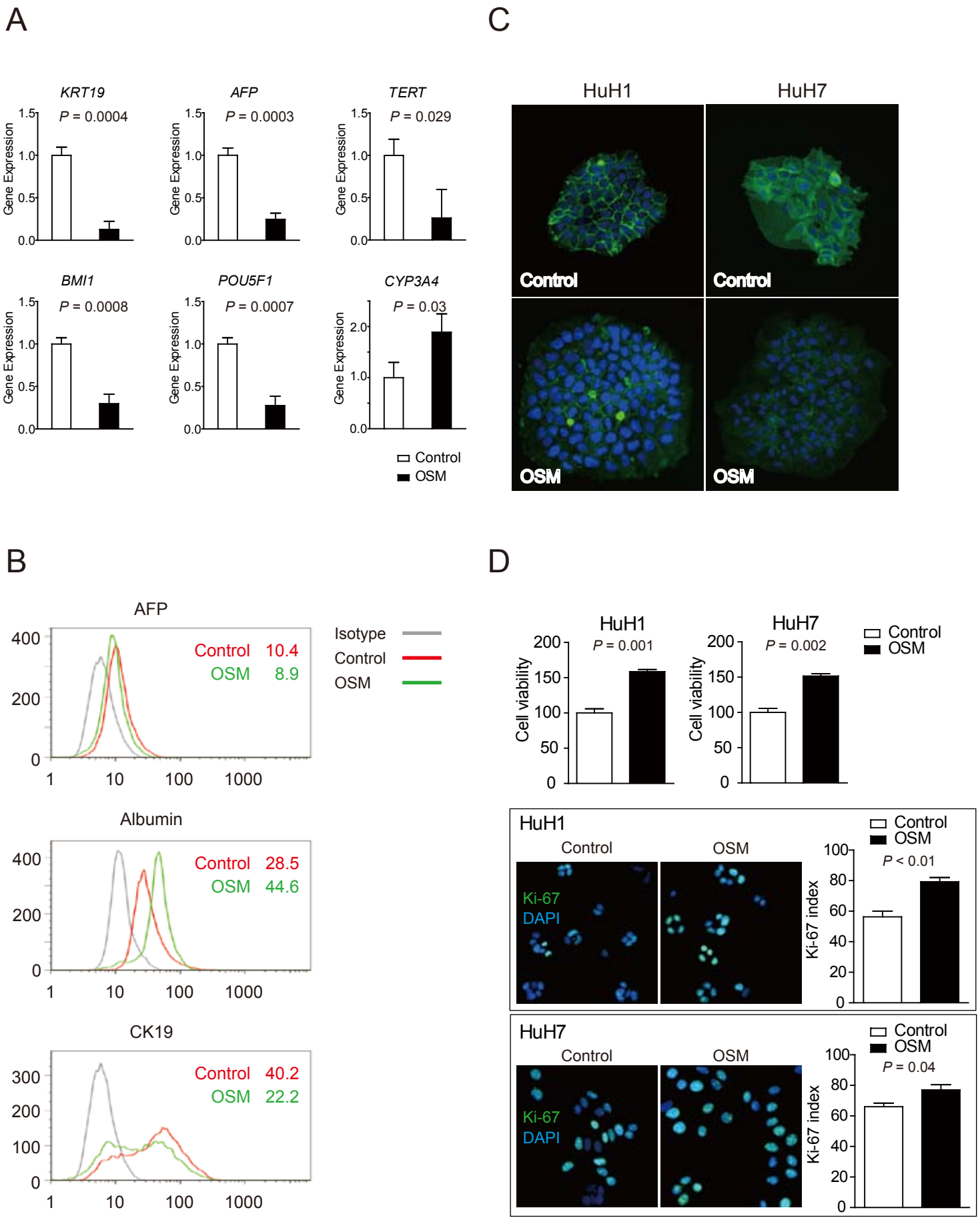
A
KRT19
P = 0.0004
AFP
P = 0.0003
TERT
P = 0.029
BMI1
P = 0.0008
POU5F1
P = 0.0007
CYP3A4
P = 0.03
Gene Expression
Control
OSM
C
HuH1
HuH7
Control
Control
OSM
OSM
B
AFP
Control 10.4
OSM 8.9
Isotype
Control
OSM
Albumin
Control 28.5
OSM 44.6
CK19
Control 40.2
OSM 22.2
D
HuH1
P = 0.001
HuH7
P = 0.002
Cell viability
Control
OSM
HuH1
Control
OSM
Ki-67
DAPI
P < 0.01
Ki-67 index
HuH7
Control
OSM
Ki-67
DAPI
P = 0.04
Ki-67 index

Figure 4

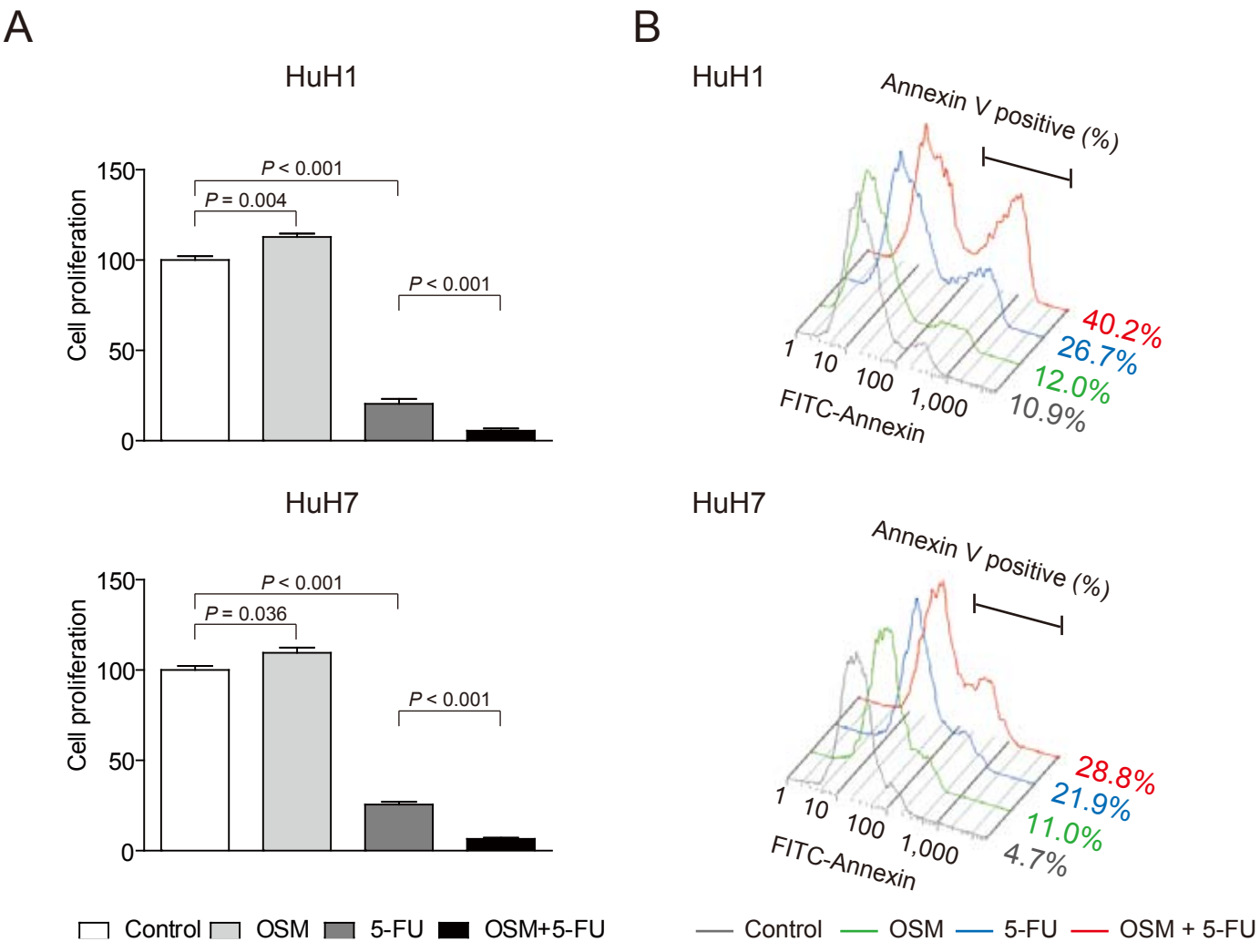
A
HuH1
Cell proliferation
150
100
50
0
P < 0.001
P = 0.004
P < 0.001
HuH7
Cell proliferation
150
100
50
0
P < 0.001
P = 0.036
P < 0.001
Control
OSM
5-FU
OSM+5-FU
B
HuH1
Annexin V positive (%)
1
10
100
1,000
FITC-Annexin
40.2%
26.7%
12.0%
10.9%
HuH7
Annexin V positive (%)
1
10
100
1,000
FITC-Annexin
28.8%
21.9%
11.0%
4.7%
Control
OSM
5-FU
OSM + 5-FU

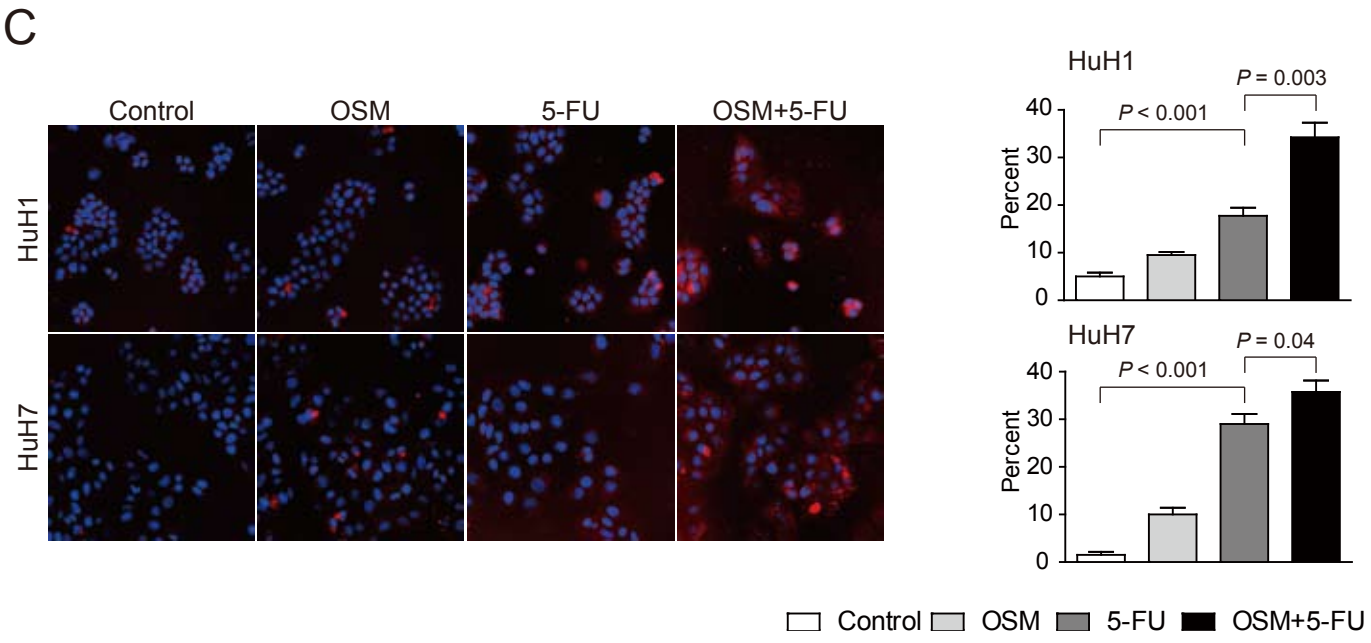
C
Control
OSM
5-FU
OSM+5-FU
HuH1
HuH7
HuH1
Percent
40
30
20
10
0
P < 0.001
P = 0.003
HuH7
Percent
40
30
20
10
0
P < 0.001
P = 0.04
Control
OSM
5-FU
OSM+5-FU

Figure 5

A

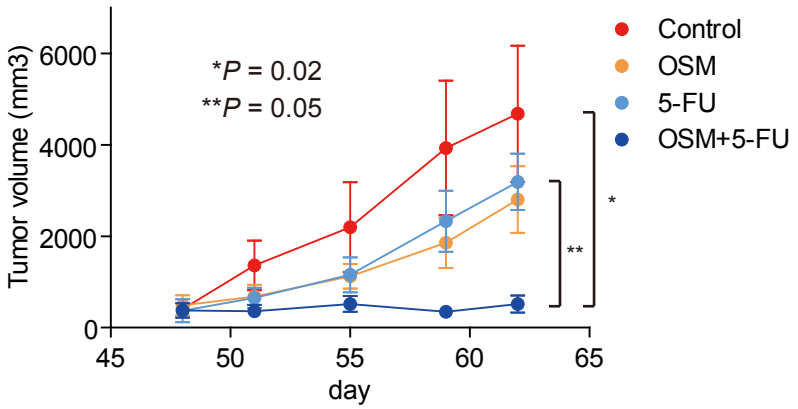
Tumor volume (mm3)
6000
4000
2000
0
45
50
55
60
65
day
*P = 0.02
**P = 0.05
Control
OSM
5-FU
OSM+5-FU
*
**

B

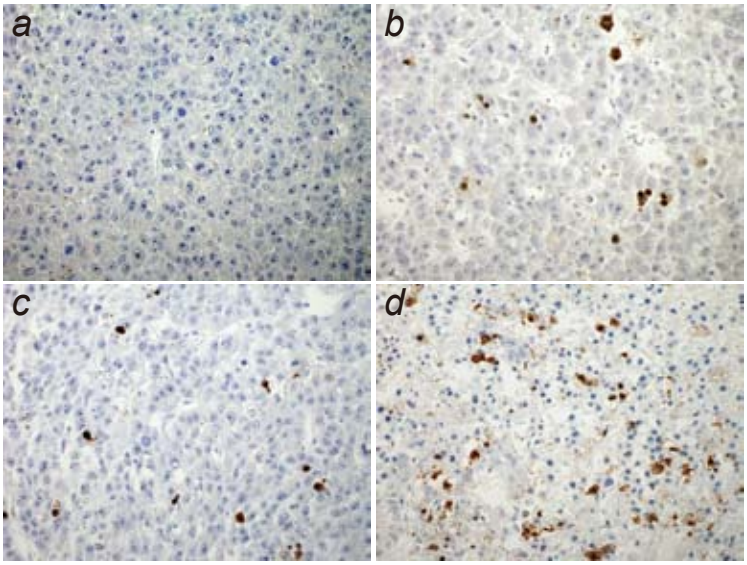
a
b
c
d

C

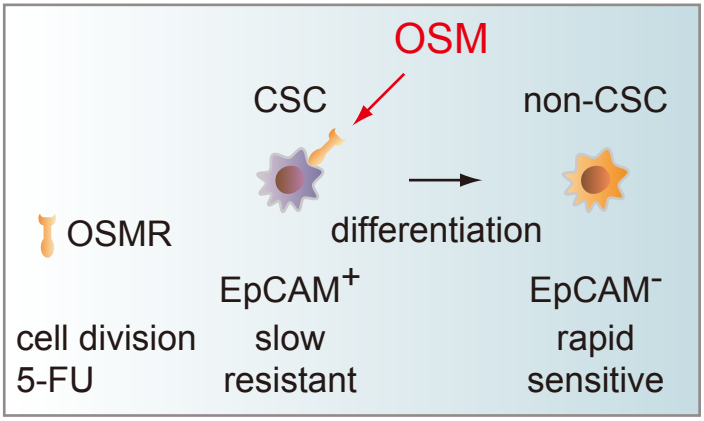
OSM
CSC
non-CSC
OSMR
differentiation
EpCAM+
EpCAM-
cell division
5-FU
slow
resistant
rapid
sensitive

Supplemental Figure 1

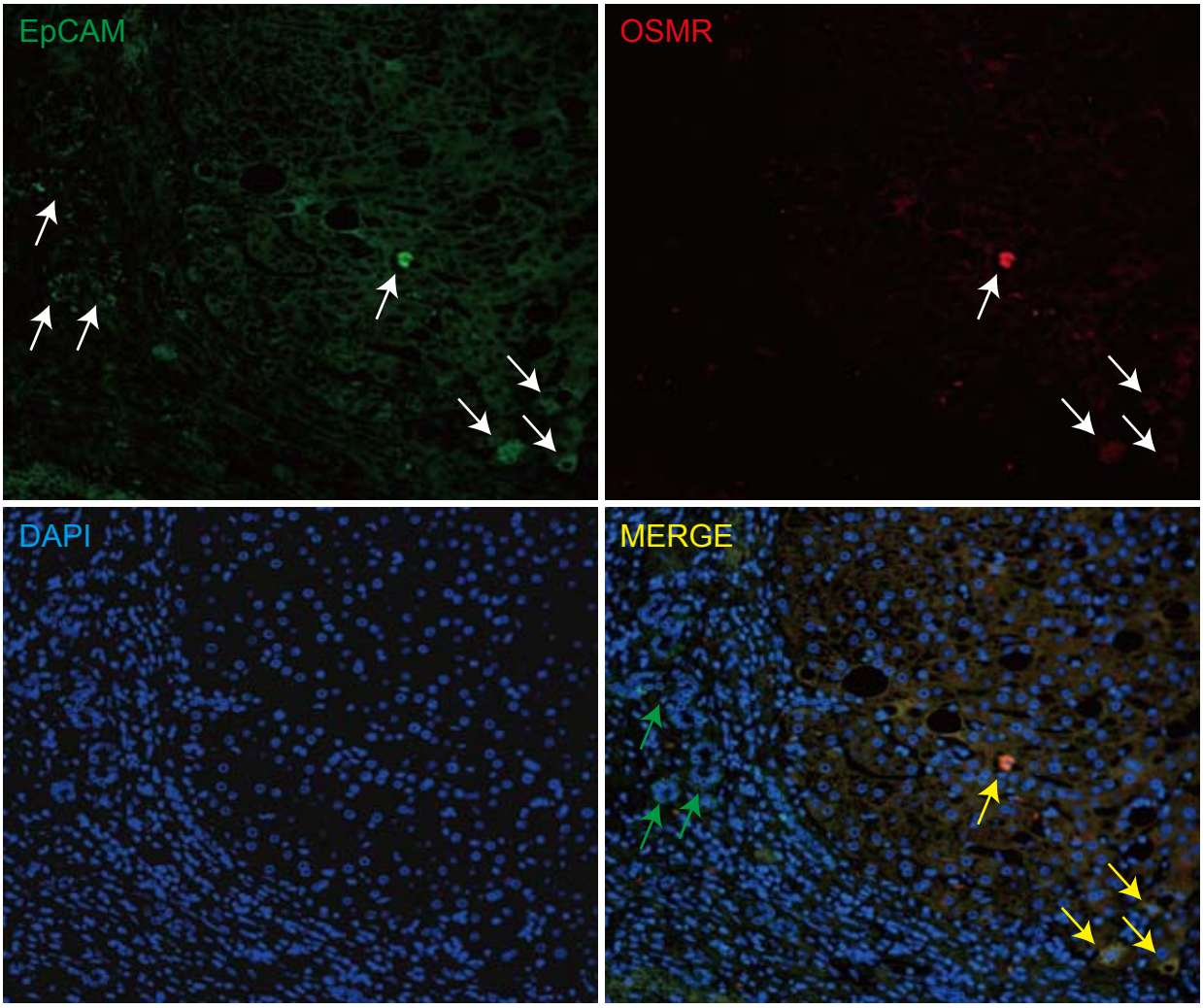

Supplemental Figure 2

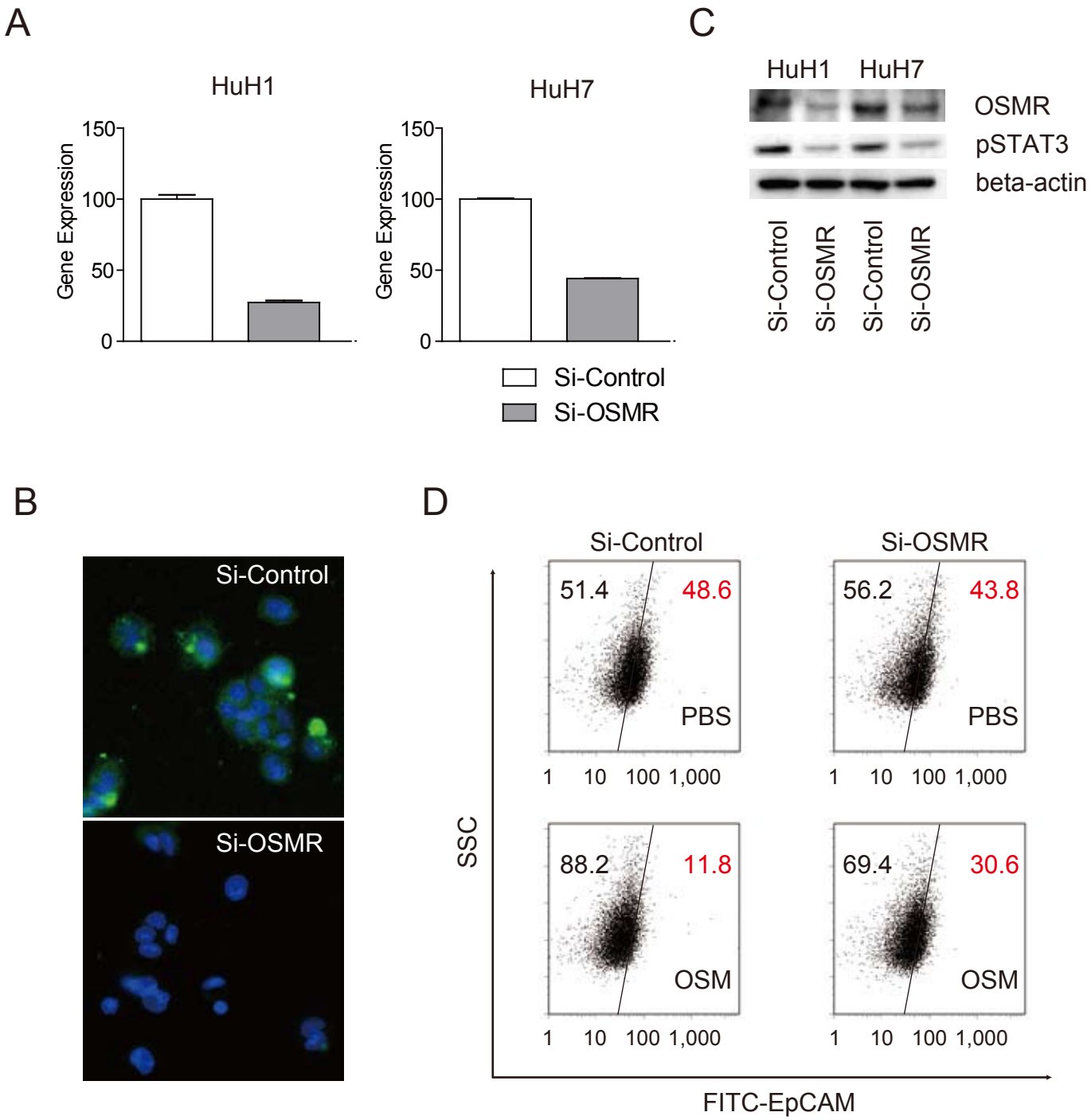

Supplemental Figure 3